

Pressure-induced transformations and high-pressure behaviour in cyanoadamantane plastic crystal

This article has been downloaded from IOPscience. Please scroll down to see the full text article.

2003 J. Phys.: Condens. Matter 15 8647

(<http://iopscience.iop.org/0953-8984/15/49/033>)

View [the table of contents for this issue](#), or go to the [journal homepage](#) for more

Download details:

IP Address: 171.66.16.125

The article was downloaded on 19/05/2010 at 16:03

Please note that [terms and conditions apply](#).

Pressure-induced transformations and high-pressure behaviour in cyanoadamantane plastic crystal

Alain Hédoux, Yannick Guinet, Patrick Derollez, Jean-François Willart, Frédéric Capet and Marc Descamps

Laboratoire de Dynamique et Structure des Matériaux Moléculaires, UMR CNRS 8024, Université des Sciences et Technologies de Lille, UFR de Physique Bâtiment P5, 59655 Villeneuve d'Ascq Cedex, France

Received 11 July 2003

Published 25 November 2003

Online at stacks.iop.org/JPhysCM/15/8647

Abstract

Raman scattering investigations of cyanoadamantane (CNa) plastic crystals were performed in the 0–10 GPa pressure range. A phase transition towards an ordered high-pressure (HP) phase is clearly identified. However, this transition can be easily bypassed upon pressurization, placing the initial plastic phase in a metastable situation. Between 0.3 and 0.7 GPa the escape from metastability is observed through the isobaric transformation towards the ordered HP phase. Above 0.7 GPa, the lifetime of the metastability appears to be infinite with respect to the experimental timescale, suggesting that the glassy crystal state was reached upon pressurization. Above 10 GPa, the metastable plastic phase, as well as the ordered HP phase, convert into a conventional amorphous state. The structural features of the ordered and the glassy crystal HP phases, determined from Raman investigations, were compared to those of the ordered and glassy crystal phases usually obtained upon cooling.

1. Introduction

A great amount of interest in condensed matter physics is devoted to understanding the ability of some materials to avoid crystallization during rapid or even relatively slow cooling below their melting temperature. Such a property usually generates a glass transition connected to the intense slowing down of the molecular dynamics upon cooling. The increase of the internal molecular relaxation time is related, from Adam–Gibbs theory [1], to the growth of cooperatively rearranging regions which could be associated to the development of a structural organization. However, supercooled liquids are not very well adapted materials for structural investigations in the short range order (SRO) whereas plastic crystals [2, 3] provide better conditions for searching for structural evolution connected to the vitrification mechanism. Glassy crystals are obtained by rapid undercooling of plastic crystals in which the average position of the centres of mass are ordered on a lattice while the orientations are dynamically

disordered. This undercooling is accompanied by a considerable increase in relaxation times on approaching T_g , as observed in conventional glass formers [4].

A clear signature of cooperatively rearranging regions has been experimentally determined in cyanoadamantane [5, 6] ($C_{10}H_{15}-CN$, CNa) on approaching T_g , through the development of SRO fluctuations. These latter have been considered as the precursor of the development of a long range order (LRO) different from that in the stable low-temperature (LT) phase [6, 7]. A second route of vitrification, different from the thermal quench, is the increase of pressure. Despite the fact that the pressure required to approach the glass transition is generally very high, technological advances on membrane diamond-anvil cells (MDACs) allows very high-pressure (HP) investigations up to about 50 GPa. This kind of pressure cell is well adapted for Raman spectroscopy, which is a sensitive probe for detecting subtle structural transformations in the SRO [8, 9]. In this paper, we present Raman scattering investigations in the 0–10 GPa pressure range of CNa glassy crystals. The objective is to probe the polymorphism of this material and to test the capacity of CNa to reach a glassy state (corresponding to the freezing of the dynamical disorder in the plastic phase) under pressure. These results are expected to give a better insight into an understanding of the orientational glass transition mechanism observed by the usual thermal quench of the plastic phase.

2. Experimental details

Experiments were performed at room temperature (RT) on a single crystal of CNa grown using the sublimation method. Pressure was generated in a gasketed MDAC. Measurements were carried out without any pressure-transmitting medium. Sample size was typically 210 μm diameter and 110 μm thickness. Three ruby crystals (size $\sim 10 \mu\text{m}$) were included for *in situ* pressure measurements by the standard ruby fluorescence technique [10] with an accuracy of ± 0.1 GPa. Five pressure runs were done in the 0–1 GPa pressure range using the following procedure. The pressure was directly increased at different values ($P = 0.3, 0.4, 0.5, 0.7$ and 0.8 GPa), stabilized over the time for the experimental investigation (analysis of the time dependence of the Raman spectrum) and released. The HP behaviour of the CNa was further analysed in the 0–10 GPa pressure range from 3 (or 1, depending on the pressure programme applied) runs performed to obtain an homogeneous distribution of experimental data over the whole pressure range. Pressure measurements on the three ruby crystals indicate that pressure gradients in the sample were insignificant over the range studied (0–10 GPa). The 514.5 nm line of a mixed argon–krypton laser was used for Raman excitation. An Olympus 50 \times long-working-distance objective was used. The back-scattering spectra were recorded using a DILOR-XY spectrometer equipped with a liquid nitrogen cooled charge-coupled-device detector. Spectrometer slits were kept at 150 μm , which gives a resolution-limited width of 1.3 cm^{-1} . The 5–600 cm^{-1} frequency range was systematically investigated.

3. Results

3.1. Raman spectrum just after pressurization

Raman spectra were respectively recorded under ambient conditions (RT, P_{atm}) in the pressure cell, just after pressurizing the plastic phase (RT, $P = 0.7$ GPa) and just after a thermal quench of the plastic phase in the glassy state (170 K, P_{atm}).

The corresponding lattice mode region lying in the 0–120 cm^{-1} range is reported in figure 1. Under ambient conditions the spectrum shows the characteristic lineshape of a disordered phase, as expected for a plastic phase. Due to the molecular symmetry (C_{3v}) the

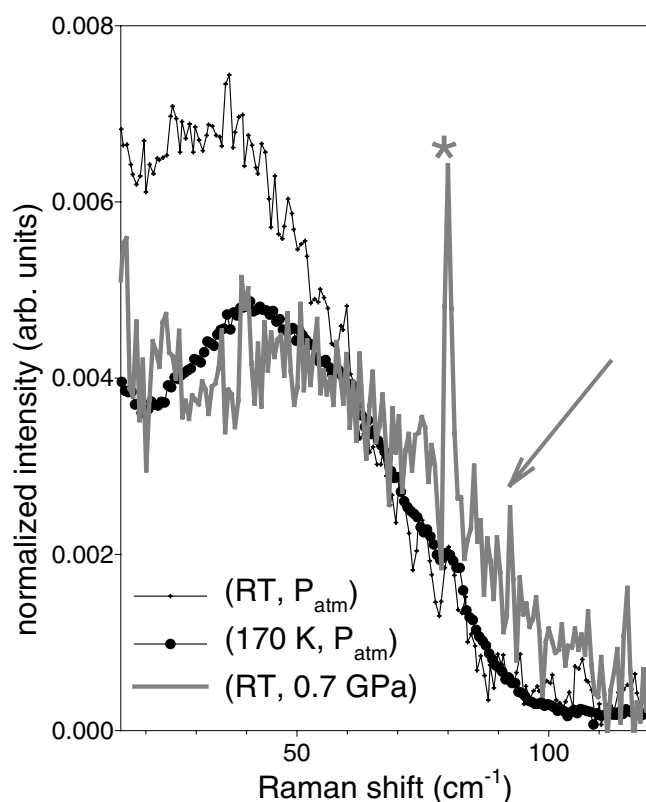


Figure 1. The low-frequency Raman spectrum of CNa under pressure (0.7 GPa) compared with the spectrum taken under ambient conditions and with that recorded in the glassy state at 170 K obtained by rapid cooling. The star indicates a plasma line.

low-frequency Raman spectrum of CNa is composed of two types of rotational motions of the C_3 molecular axis: reorientation and libration [11]. Only rotational motions of the molecular axis have a contribution to the anisotropy of the polarizability tensor [11] responsible for the inelastic Raman activity. Reorientations of the molecular axis lead to a quasi-elastic component in the very-low-frequency range ($\omega < 10 \text{ cm}^{-1}$) while librations correspond to a low-frequency broad band. The broad lineshape of the librational band corresponds to a distribution of frequencies of C_3 -axis librations inherent in the orientational molecular disorder. Consequently the broad low-frequency band reflects the density of states of the C_3 molecular librations through the relation [12]

$$I_{\text{Ram}}^{\text{obs}} \propto \left[1 - \exp\left(-\frac{\hbar\omega}{kT}\right) \right] \frac{C(\omega)G_L(\omega)}{\omega}$$

where $C(\omega)$ and $G_L(\omega)$ are, respectively, the photon–phonon coupling coefficient and the librational density of states.

Under pressure a similar Raman spectrum with non-resolved phonon peaks is observed, which clearly indicates that pressurized CNa at 0.7 GPa is not in an ordered state. Moreover, the phonon density of states becomes much broader due to the development of a shoulder on the high frequency side (localized by an arrow on figure 1). This broadening reveals that the orientational disorder persists under pressure.

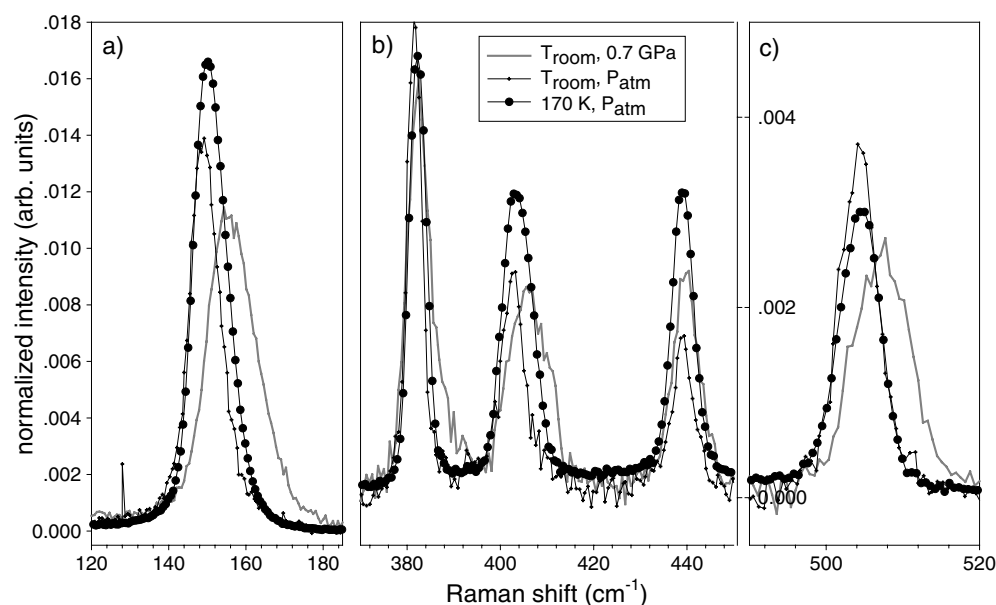


Figure 2. The high-frequency spectrum in the 120–520 cm^{-1} range of the disordered HP state, the rotator phase under ambient conditions and the glassy state at 170 K.

The low-frequency spectra taken in the pressure cell under ambient conditions and after pressurization at 0.7 GPa are compared in figure 1 to the spectrum of the glassy state recorded just after a rapid cooling from RT down to 170 K. This comparison shows a similar band shape for the low-frequency librational band recorded in the glassy state and in the disordered compressed state.

The internal mode region lying in the range 120–520 cm^{-1} is reported in figure 2 for the three spectra taken at RT under ambient pressure and at 0.7 GPa, and under ambient pressure at 170 K in the glassy state ($T_g = 175$ K). The most intense band near 150 cm^{-1} (figure 2(a)) corresponds to the bending mode, i.e. the C–C \equiv N distortion with respect to the C_3 -molecular axis [13]. For each spectrum this Raman band is highly asymmetric. At RT these features have been assigned, in a previous study [13], to the existence of two components reflecting a SRO since only one component is expected from symmetry considerations. From x-ray diffraction experiments [3], this SRO was determined as a predictor of an antiferroelectric order of molecules along one of the four-fold cubic axes. This latter is different from the antiferroelectric order of molecular dipoles along one of the cube diagonal's directions that ultimately develops in the LT monoclinic phase [14]. The concomitant observation of the asymmetric lineshape of the bending band in the HP spectrum can thus reasonably be considered as the manifestation of the SRO detected in the plastic phase at RT and in the undercooled plastic phase.

The most striking feature observed in the spectrum of internal modes (figures 2(a)–(c), table 1) is a systematic broadening of the Raman bands of CNa when the pressure increases while a slight sharpening or a quasi-independent temperature behaviour of these bands is observed when the temperature is decreased. On the other hand, no systematic pressure effect on the frequency of the internal Raman bands is observed. The Raman bands near 150, 405 and 505 cm^{-1} shift with increasing pressure, whereas near 380 and 440 cm^{-1} no pressure-induced frequency shift is observed in the 0–0.7 GPa range.

Table 1. FWHM of internal lines determined by a fitting procedure carried out in different disordered states depending on experimental conditions; the plastic state under ambient conditions, the glassy state obtained by rapid cooling below $T_g = 175$ K and the over-compressed state obtained by direct pressurization at 1 GPa, and then pressurized at 2.3 GPa.

	RT, P_{atm}	170 K, P_{atm}	RT, 2.3 GPa
	Plastic phase	Glassy state	Over-compressed plastic phase
Internal lines			
ω (cm^{-1}) at RT, P_{atm}	FWHM (cm^{-1})	FWHM (cm^{-1})	FWHM (cm^{-1})
147.3	5.8 ± 0.1	5.3 ± 0.2	15.6 ± 0.7
151.0	7.4 ± 0.1	7.5 ± 0.2	15.1 ± 0.8
380.0	3.4 ± 0.1	3.0 ± 0.1	7.5 ± 0.2
401.0	4.0 ± 1.2	3.9 ± 0.4	10.4 ± 0.7
402.8	6.5 ± 0.2	4.9 ± 0.4	5.0 ± 0.9
438.6	6.4 ± 0.2	4.4 ± 0.1	8.4 ± 0.2
502.6	4.8 ± 0.4	3.8 ± 0.4	12.0 ± 0.8
504.0	3.6 ± 0.4	3.4 ± 0.4	5.8 ± 0.8
545.0	3.7 ± 1.0	4.4 ± 0.7	7.6 ± 1.0

3.2. Temporal evolution of the Raman spectrum after pressurization

At $P = 0.7$ GPa an isobaric transformation of the Raman spectrum is clearly observed both in the low-frequency and high-frequency regions (figure 3). The broad low-frequency librational band sharpens continuously until the observation of four phonon peaks (figure 3(a)). Such a structuring of the low-frequency Raman spectrum into phonon peaks can be interpreted as the development of a LRO and then suggests a pressure-induced ordering. The asymmetric bending band (observed in figure 2(a)) splits into three components (figure 3(a)). At higher frequency (figure 3(b)) spectral changes are localized around 405 and 505 cm^{-1} . In the first region (405 cm^{-1}) a splitting of the Raman band is observed, while a contribution to the Raman band at 505 cm^{-1} disappears during the transformation. These features will be analysed further.

After 200 min, as the pressure is released step by step, the transformation of the ordered phase into the disordered plastic phase was observed between 0.3 and 0.2 GPa. After a direct pressurization of CNa in the 0.4–0.7 GPa pressure range, an isobaric transformation (similar to that described above at $P = 0.7$ GPa) is systematically observed. Consequently it can be assumed that, above 0.3 GPa, CNa is placed in a metastable disordered state. This state was then called the over-compressed disordered state.

3.3. Analysis of the ordered high-pressure (HP) phase

Figure 4 shows the Raman spectra of both the HP phase and the LT phase which has been obtained by isothermal ageing at 220 K and cooled at 100 K where phonon peaks appear more resolved. Despite the poor quality of the low-frequency spectrum of the HP phase compared with that of the LT phase, the two spectra can be reasonably considered as different from the observation of the following features.

- In the lattice mode region the best fit of the HP spectrum is obtained using four damped oscillators indicated by grey arrows in figure 4(a). A similar fitting procedure of the LT spectrum reveals six Raman-active modes, in agreement with a previous study [13]. Consequently the symmetry of the HP phase is higher than that of the $C2/m$ symmetry of the LT phase [14].

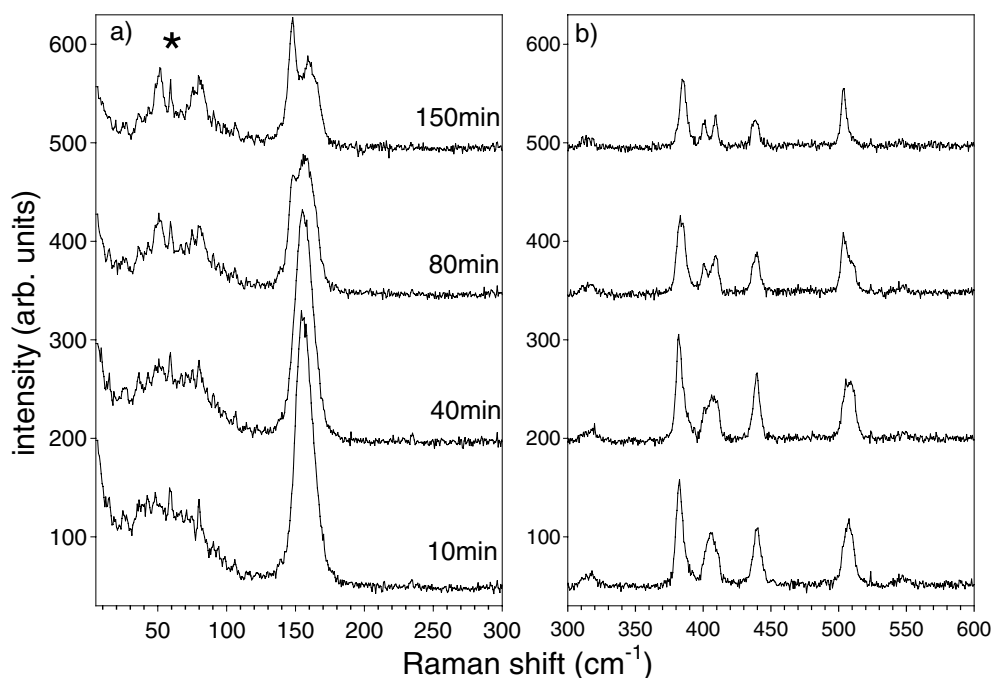


Figure 3. The time dependence of the Raman spectrum of CNa pressurized at 0.7 GPa. The star indicates a plasma line.

- In the internal mode region [$120\text{--}600\text{ cm}^{-1}$], the number of internal modes in the HP phase is higher than in the LT phase. Consequently the site symmetry in the HP phase is lower than the C_{1h} symmetry in the LT phase [13, 14]. In the bending mode region (figure 4(b)), three components are detected in the spectrum of the HP phase, whereas only two components ($1A_g + 1B_g$) are expected and observed in the LT phase. Taking into account the high sensitivity to probe the local organization of molecular dipoles [13] through the numbering or lineshape of the bending bands, the detection of three bending peaks indicates that the orientational LRO in the HP phase is different from that determined in the monoclinic LT phase [14].

Consequently the comparison of Raman spectra of the LT and HP phases over a wide spectral window (lying both in the lattice- and internal-mode regions) demonstrates indubitably that these ordered phases are different.

3.4. High-pressure dependence of CNa

When the pressure is directly increased from atmospheric pressure to above 0.7 GPa, no transformation of the Raman spectrum was observed over a timescale of about 30 days. Consequently in such conditions the HP behaviour of the over-compressed disordered state can be investigated and compared to that of the HP ordered phase (obtained after the isobaric transformation at 0.7 GPa) over the 0–10 GPa pressure range. The pressure dependence of the Raman spectra in the disordered and ordered states of CNa are reported in figures 5(a) and (b) in the $5\text{--}300\text{ cm}^{-1}$ low-frequency region and in figures 6(a) and (b) in the $300\text{--}600\text{ cm}^{-1}$ range to give a clear description of pressure effects.

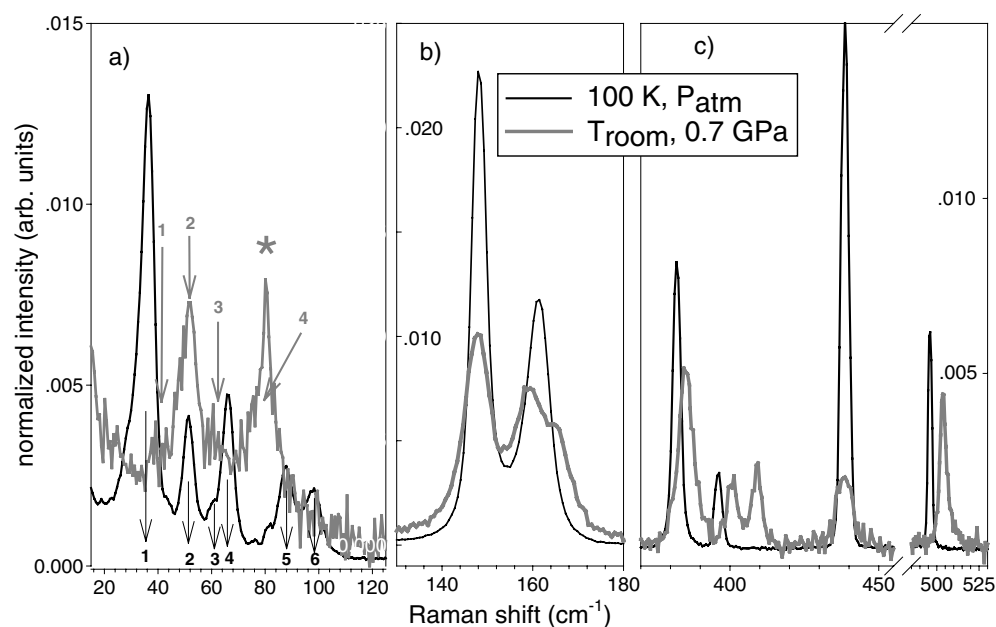


Figure 4. Raman spectra of the ordered HP (RT, 0.7 GPa) and LT (100 K, P_{atm}) phases. Grey and black arrows and associated numbers indicate the numbering of lattice modes in the HP and LT ordered phases, respectively.

Pressurization of the over-compressed disordered state from 1 up to 10 GPa was performed in one pressure run. In the 5–300 cm^{-1} range, significant pressure-induced frequency shifts of the broad librational band and the bending band are observed. These frequency shifts are accompanied by unusual broadenings. Above 3 GPa the low-frequency band and the bending band overlap. A splitting of the bending band is observed in the 5–8 GPa pressure range while the low-frequency band remains very broadened. Above 8 GPa, internal bending modes lose their splitting and the contributions of the low-frequency band and the bending band are indistinguishable one from the other. In the 300–600 cm^{-1} range, internal lines weaken and broaden with increasing pressure. The linked observations of a much broadened band in the low-frequency range and the special pressure behaviour of internal modes in the 300–600 cm^{-1} range suggest that the cubic lattice in the over-compressed plastic crystal has broken down. From these experiments no ordering process was observed after pressurizing the over-compressed disordered state.

Pressurization of the HP ordered phase was performed on two pressure runs, to reach 10 GPa with a homogeneous distribution of measurements over the 1–10 GPa pressure range. The sample was first pressurized in the 0.3–0.7 GPa pressure range and annealed to obtain the ordered state after the isobaric transformation of the metastable disordered state. In the low-frequency range strong pressure dependences of the Raman frequencies are observed both for the lattice modes and the bending bands. Drastic broadenings of the Raman bands with concomitant decreases of intensities are also observed. Only the two most intense phonon peaks (localized by arrows in figure 5(c)) merging into the background can be identified at 4.5 GPa. At 10 GPa (figure 5(d)) the overlapping of phonon peaks and bending bands are also observed. Despite the observation of some structure in the low-frequency Raman lineshape, the weak intensity and the broadening of the lattice modes suggest a crystalline-to-amorphous

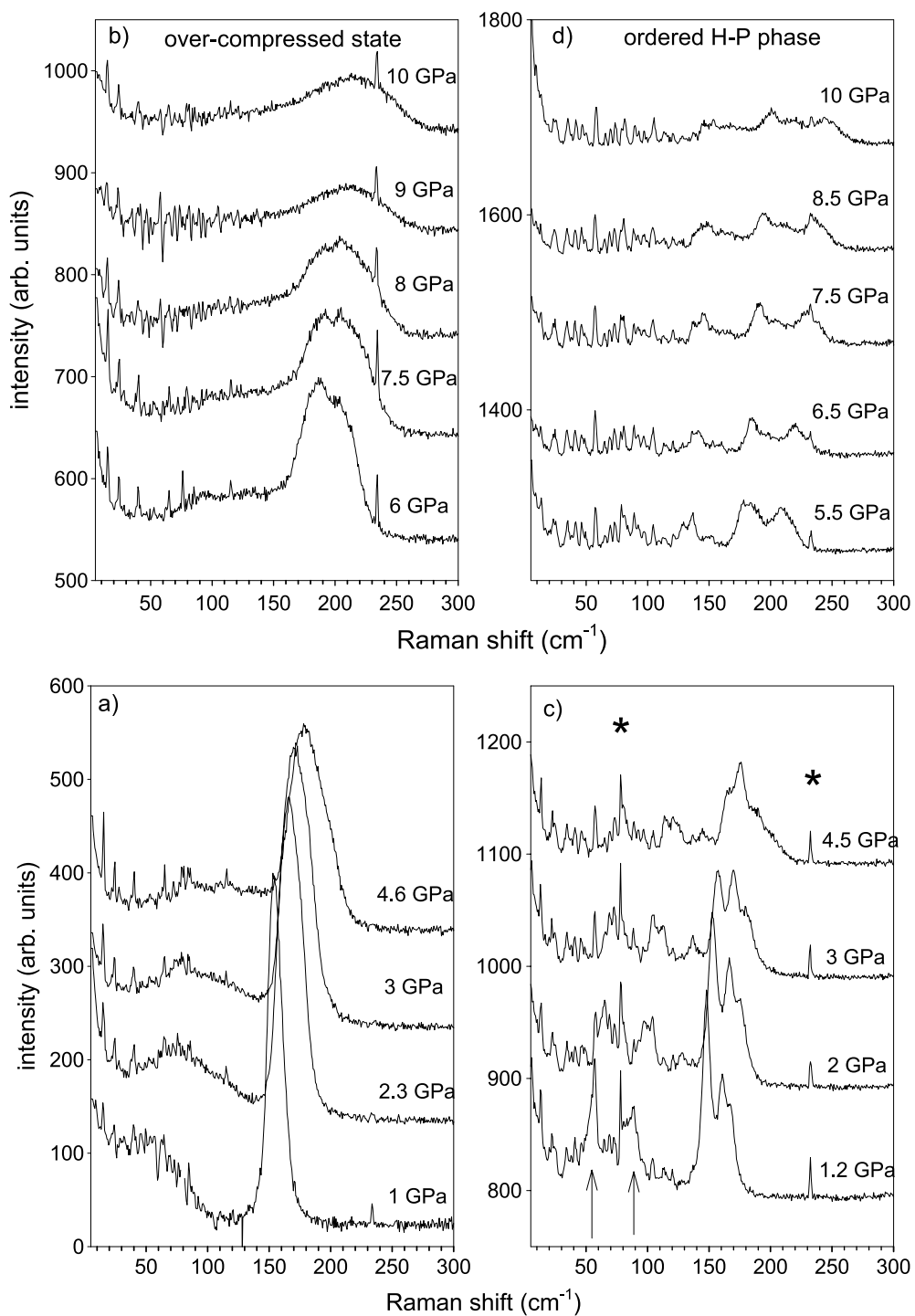


Figure 5. Pressure dependence of the Raman spectra in the 5–300 cm^{-1} frequency range recorded during the pressurization of the over-compressed state (a) and (b), and during pressurization of the ordered HP phase (c) and (d). Stars indicate plasma lines.

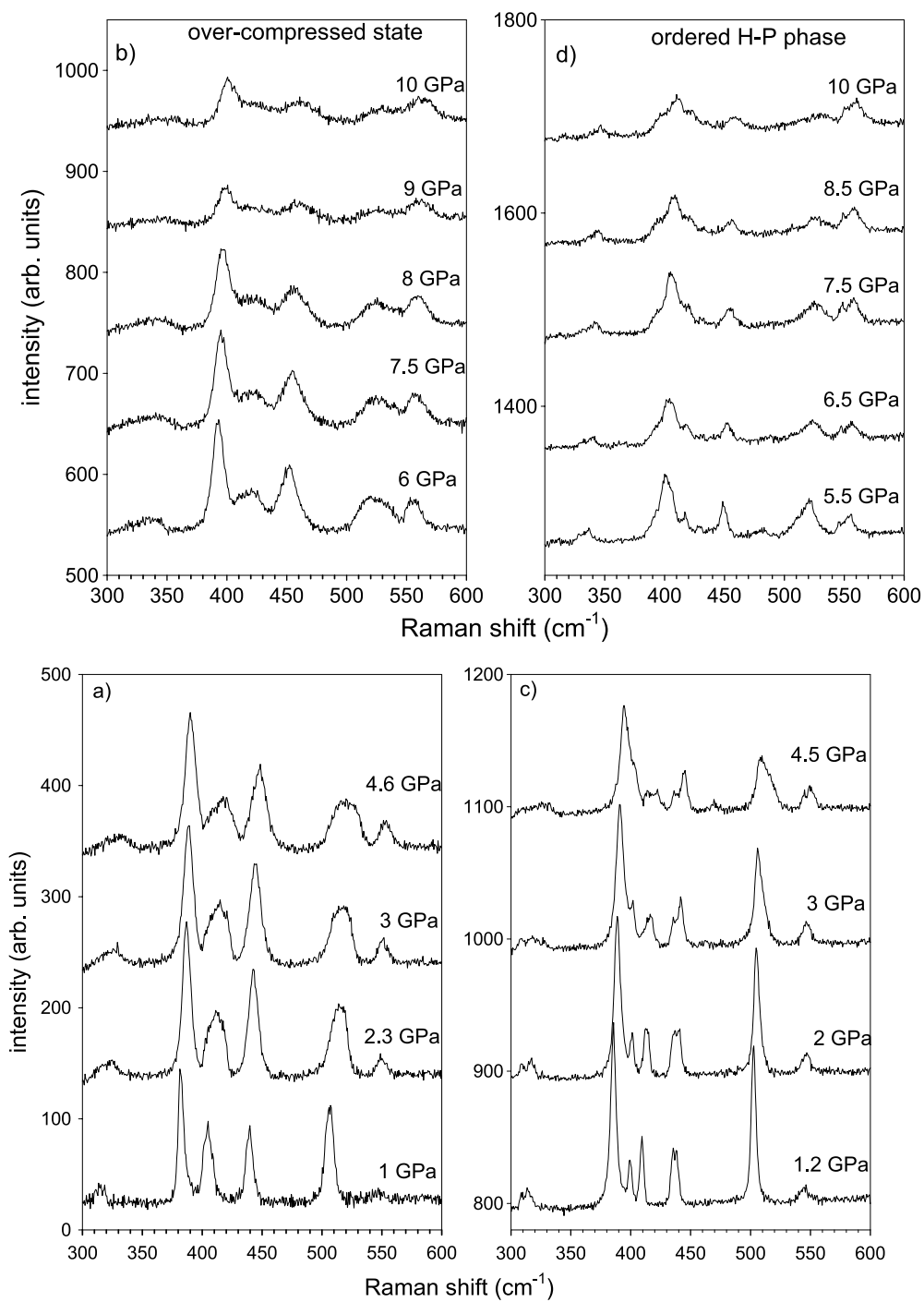


Figure 6. Pressure dependence of the Raman spectra in the 300–600 cm^{-1} frequency range recorded during the pressurization of the over-compressed state (a) and (b), and during pressurization of the ordered HP phase (c) and (d).

transition. Additional evidence for this transition is also found in the internal mode region (figure 6) where relatively sharp peaks (at low pressure) around 380 and 500 cm^{-1} are observed with increased width and weaker intensities above 4.5 GPa.

The qualitative analysis of the pressure dependence of the HP ordered and over-compressed disordered phases is performed from the comparison of the Raman spectra taken during pressurization of the HP ordered phase and the over-compressed disordered state, in the 5–300 cm^{-1} and 300–600 cm^{-1} ranges (figures 5 and 6). This analysis highlights several original features.

- A broadening of the Raman lineshape is observed in the 5–600 cm^{-1} range as soon as the sample is pressurized both from the disordered and ordered states. The broadening of internal modes indicates a widening of the distribution of molecular surroundings with pressurization.
- The low-frequency spectrum taken after pressurization of the disordered state (figure 5(b)) appears as the envelope of Raman bands in the spectrum of the HP ordered phase. At higher frequencies (figures 6(b), (d)) the Raman spectra taken are very similar.

Consequently pressurization of the over-compressed disordered state or the ordered HP phase promotes disorder and leads to a single amorphous state. Figures 5 and 6 display two different (ordered or disordered) crystal-to-amorphous transitions leading to a quasi-similar description of the amorphous state. Pressure-induced amorphizations have been observed in many other compounds [15–27], among which are several recognized to be typical molecular crystals [15–21]. However, the evidence for two different routes to a single amorphous state is unusual.

4. Analysis and discussion

After pressurization of the plastic phase in the 0.3–0.7 GPa range a time-dependent transformation is systematically observed. The structuring of the broad librational band into phonon peaks and the splittings of internal lines indubitably reveal the achievement of the HP orientational LRO. Upon release of pressure, the order–disorder phase transition was observed below 0.3 GPa, indicating that CNa is placed in a metastable over-compressed disordered state above 0.3 GPa. This is the first experimental evidence for a time-dependent ordering process under pressure, and also for a metastable over-compressed disordered state in plastic crystals. Taking into account that the materials which can be easily undercooled are usually glass formers, one can expect a glass transition under pressure for CNa plastic crystals, as observed for molecular liquids [28, 29], since CNa can be over-compressed. In this context, the infinite lifetime of the metastability of the disordered state pressurized above 0.7 GPa suggests that the glassy crystal state is reached.

The analysis of Raman features observed during the isobaric ageing in the bending mode region (150–220 cm^{-1}), around 405 and 505 cm^{-1} , was reported in figure 7. The Raman lineshape is fitted using damped oscillators by the residue method. Figures 7(a)–(c) exhibit a plateau of about 40–50 min in the time dependence of three independent quantities. This induction time strongly suggests that the transformation of the metastable plastic phase toward the ordered HP phase occurs through a nucleation and growth process. The ordered HP phase is clearly different from the stable LT phase, suggesting two different ordering processes, by cooling and pressurization, leading to two different LRO.

Previous LT diffraction experiments [3] have already revealed two different ordering processes after a rapid quench, depending on the depth of the quench. After shallow quenches ($T \geq 200$ K), the ordering process is characterized by sigmoidal growth curves corresponding

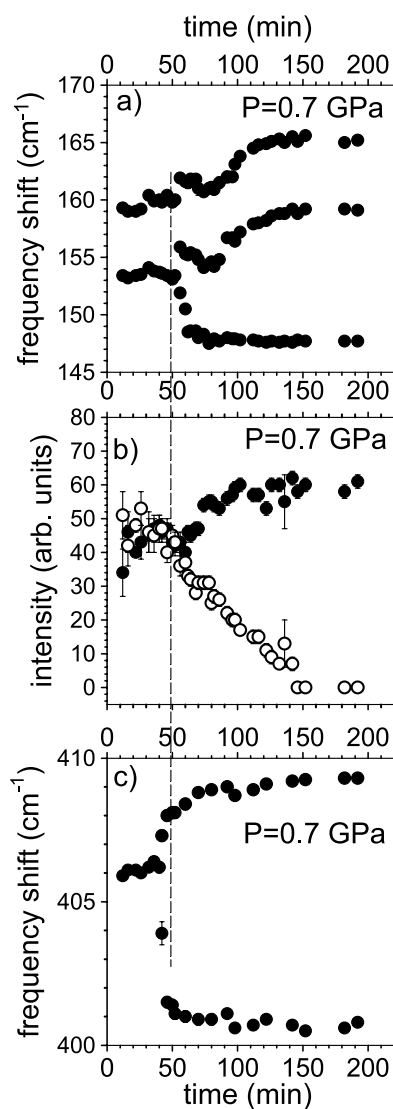


Figure 7. The time dependence of (a) Raman band frequencies in the bending-mode region, (b) Raman band frequencies around 405 cm^{-1} , (c) intensities of Raman bands around 500 cm^{-1} (full circles) and 505 cm^{-1} (open circles).

to the nucleation and growth of the ultimately monoclinic LRO. For deep quenches (below 200 K) atypical kinetic laws are observed. In this case the SRO detected at RT (in the plastic phase) persists and develops, in a first stage, upon quenching. The development of this SRO is a precursor of metastable states composed of nano-domains characterized by a LRO, different from that of the LT monoclinic phase, in the matrix of a non-transformed plastic phase. In a second stage, this transient LRO isothermally transforms into the ultimately stable monoclinic phase. Both Monte Carlo simulations and x-ray diffraction experiments [7] suggest an orthorhombic transient LRO. However, structural refinements cannot be carried out to determine the nature of this transient LRO, since it is spatially confined in nano-domains

coexisting with domains of the plastic phase. It is worth noticing that the deeper the quench, the more developed the transient LRO and the longer the ordering process. Consequently it can be reasonably assumed that the increase of strains on nano-domains, by decreasing temperature, corresponds to a local pressurization which promotes the development of the transient LRO. These considerations suggest that pressurization of CNa promotes an ordering process leading to the LRO of the HP ordered phase, which could be the transient orthorhombic LRO detected at LT.

The behaviour of CNa under pressure contrasts with that of Cla (chloroadamantane, $C_{10}H_{15}Cl$) which cannot be undercooled. Recent investigations into Cla [30, 31] have shown the existence of a HP phase (above 0.6 GPa) which is rigorously identical to the ordered LT phase. The inability of Cla to be undercooled and vitrified and the existence of only one ordered phase support the idea that the existence of two different ordered (HP and LT) phases in CNa could have an influence on the glass formation of this plastic crystal. At LT, the development of a local structure related to the HP phase hinders unavoidably the evolution of the system toward its ultimately stable phase. This frustration obviously promotes the vitrification of the system.

The Raman spectra of the over-compressed disordered state taken on pressurization, step by step, appear as the envelope of the external and internal modes of the HP ordered phase. Raman investigations both in the disordered and ordered HP states reveal clearly a systematic broadening of external and internal bands with pressurization. This behaviour is different from that observed in Cla where any significant broadening of Raman bands was detected in the ordered phase below 5 GPa. Consequently pressurization of the HP ordered phase and over-compressed disordered state of CNa promotes instantaneously disorder toward a single non-crystalline state, since Raman spectra are observed to be similar above 8 GPa (figures 5(b), (d) and 6(b), (d)).

The low-frequency spectrum of the ordered phase is greatly broadened. However, it is more structured than that of the over-compressed disordered state. This latter reflects a highly disordered organization, since no trace of LRO can be detected, in contrast to the structural description of the glassy crystals in which the average positions of the molecular centres of mass form a periodic lattice. From line transitions determined by calorimetric investigations performed on the so-called fragile molecular liquid (m-fluoroaniline) [28] it can be speculated that over-compressed CNa above 0.3 GPa corresponds to the glassy state. The strong similarity between low-frequency Raman lineshapes of the over-compressed state and the LT glassy state (figure 1) supports this consideration. Consequently the over-compressed state should be composed of domains characterized by the LRO of the HP ordered phase, since the development of the transient orthorhombic LRO was observed in the LT glassy state [7]. The consideration that this LRO is not the ultimately stable state of CNa could explain that the compression of the over-compressed and HP ordered states leads to the same non-crystalline state.

The pressure dependence of the internal mode frequencies are determined in the ordered and disordered states from a fitting procedure based on the residue method with damped oscillators. The results are plotted in figure 8. Only the two most intense phonon peaks of the ordered phase could have been fitted over the 0–4.5 GPa range. Their pressure dependence over this pressure range is linear and their slopes are reported in table 2. Figure 8 displays linear ω - P plots fitted by linear regression. The results obtained in the HP ordered phase are given in table 2. In figure 8 parallel or quasi-parallel pressure dependences are observed for Raman bands recorded by pressurizing of the ordered state and the over-compressed disordered state. Some irregularities are systematically observed in ω - P plots around 5 GPa, corresponding to a poor overlapping of the two pressure runs carried out in the HP ordered

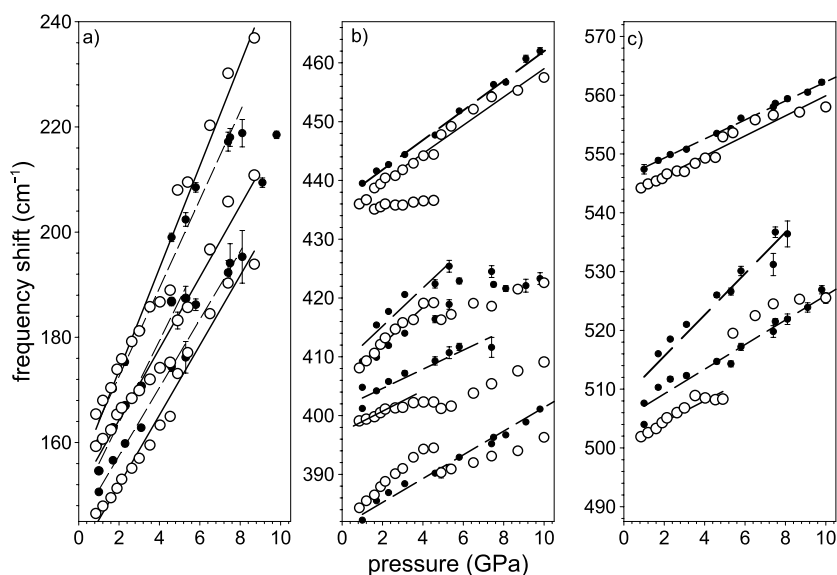


Figure 8. Pressure dependence of internal mode frequencies in the 0–10 GPa pressure range. Open circles correspond to experimental data obtained by pressurization of the ordered state and full circles by pressurization of the over-compressed state. Lines represent the linear regression of ω – P plots; broken lines correspond to full circles and full lines to open circles.

Table 2. Frequencies ω and $d\omega/dP$ of Raman lines in the ordered HP phase of CNa.

$\omega(P = 0)$ (cm^{-1})	$d\omega/dP$ ($\text{cm}^{-1} \text{GPa}^{-1}$)	Assignment
47.2	7.9(6)	External
74.0	12.1(4)	External
141.8	6.5(1)	Internal bending bands
147.9	7.8(1)	
155.8	8.4(1)	
383.1	1.9(2)	Internal
402.2	1.6(2)	—
408.9	3.2(7)	—
437.8	2.5(2)	—
501.5	2.1(1)	—
505.7	3.5(3)	—
543.3	1.6(1)	—

phase. Different orientations of the micro-domains analysed by micro-spectroscopy could be responsible for such anomalies.

From table 2, the values of the slopes of the ω – P plots are much smaller for internal modes than for lattice modes. However, they are significantly higher compared to the usual values determined for ω – T plots. One can notice from table 2 and figure 8 the rapid change of frequency of internal bending bands compared with other internal modes. This special pressure behaviour of bending modes was also observed in Cla. This confirms the high sensitivity of these vibrations to the molecular neighbourhood. The difference in pressure behaviour of frequencies between the internal and external modes is related to the large disparity between the nature of the inter- and intra-molecular interactions in molecular crystals. This disparity

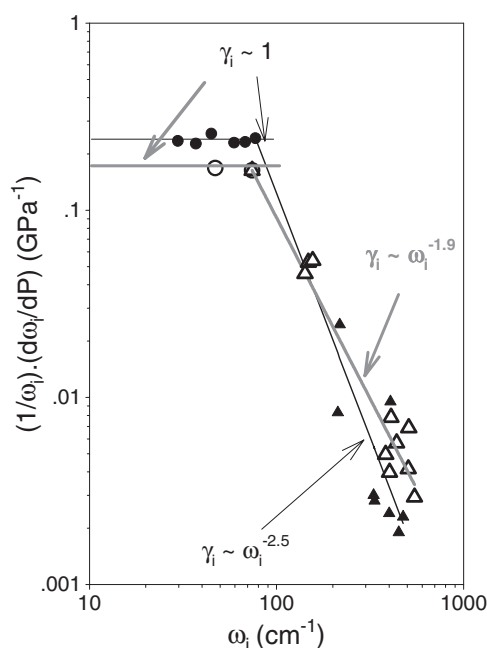


Figure 9. Vibrational scaling behaviour of CNa and Cla. Open circles and triangles correspond, respectively, to the external and internal modes in CNa and the full circles and triangles correspond to the same species of Cla.

can be visualized in figure 9, where two different pressure behaviours are observed according to the nature of the internal or external modes. Figure 9 is the log–log presentation of $(1/\omega)(d\omega/dP)$ against the zero-pressure frequency for each mode. The horizontal line is observed and expected in the external-mode regime, reflecting the $(\gamma_i \sim 1)$ behaviour of the Gruneisen parameter, while the value of -1.9 determined for the slope in the internal-mode regime reflects fairly well the expected universal behaviour $\gamma_i \sim \omega^{-2}$ in the molecular crystal [32, 33]. The experimental data obtained on CNa are compared to those obtained on Cla. This comparison shows a satisfactory agreement between the two data files. One will note, however, a notable variation with the expected law $(\gamma_i \sim \omega^{-2})$ in the case of Cla which could be related to the significant disorder of the compound.

5. Conclusion

This paper reports the first evidence for a metastable over-compressed disordered state in a plastic crystal. This observation indicates that CNa could be vitrified by pressurization. New information on the polymorphism of CNa is obtained through the evidence for a HP-ordered phase different from the ultimately stable LT phase. The confrontation of these results with those obtained on Cla suggests that the mechanism of vitrification (both by cooling and pressurization) could be connected to the development of a local structure promoted by a local pressure. Crystallographic data on the HP ordered phase are needed to give a rigorous description of the ordering process under pressure observed from these Raman spectroscopic investigations. These data should also be enlightening about the glass formation under pressure and by cooling and about the crystalline-to-amorphous transitions.

References

- [1] Adams G and Gibbs J H 1965 *J. Chem. Phys.* **43** 139
- [2] Suga H and Seki S 1974 *J. Non-Cryst. Solids* **16** 171
- [3] Descamps M and Caucheteux C 1987 *J. Phys. C: Solid State Phys.* **20** 5073
- [4] Lunkenheimer P, Schneider U, Brand R and Loidl A 2000 *Contemp. Phys.* **41** 15
- [5] Willart J F, Descamps M and Miltenburg van J C 2000 *J. Chem. Phys.* **112** 10992
- [6] Affouard F, Willart J-F and Descamps M 2002 *J. Non-Cryst. Solids* **307–310** 9
- [7] Descamps M, Willart J F, Kuchta B and Affouard F 1998 *J. Non-Cryst. Solids* **235–237** 559
- [8] Hédoux A, Guinet Y and Descamps M 1998 *Phys. Rev. B* **58** 31
- [9] Hédoux A, Denicourt T, Guinet Y, Carpentier L and Descamps M 2002 *Solid State Commun.* **122** 373
- [10] Barnett J D *et al* 1973 *Rev. Sci. Instrum.* **44** 1
- [11] Sauvajol J-L, Bée M and Amoureux J-P 1982 *Mol. Phys.* **46** 811
- [12] Rolland J P and Sauvajol J-L 1986 *J. Phys. C: Solid State Phys.* **19** 3475
- [13] Guinet Y and Sauvajol J-L 1988 *J. Phys. C: Solid State Phys.* **21** 3827
- [14] Foulon M, Amoureux J P, Sauvajol J L, Cavrot J P and Muller M 1984 *J. Phys. C: Solid State Phys.* **17** 4213
- [15] Snoke D W, Raptis Y S and Syassen K 1992 *Phys. Rev. B* **45** 14419
- [16] Chandrabhas N, Sood A K, Muthu D V S, Sundar C S, Bharathi A, Hariharan Y and Rao C N R 1994 *Phys. Rev. Lett.* **73** 3411
- [17] Deb S K, Rekha M A, Roy A P, Vijaykumar V, Meenakshi S and Godwal B K 1993 *Phys. Rev. B* **47** 11491
- [18] Sugai S 1985 *J. Phys. C: Solid State Phys.* **18** 799
Fujii Y, Kowaka M and Onodera A 1985 *J. Phys. C: Solid State Phys.* **18** 789
- [19] Chaplot S L, Mierzezejewski A and Pawley G S 1985 *Mol. Phys.* **56** 115
- [20] Chaplot S L and Mukhopadhyay R 1986 *Phys. Rev. B* **33** 5099
- [21] Zhang D, Lan G, Hu S, Wang H and Zheng J 1995 *J. Phys.: Condens. Matter* **56** 27
- [22] Arora A K and Sakuntala T 1992 *J. Phys.: Condens. Matter* **4** 8697
- [23] Winters R R, Serghiou G C and Hammack W S 1992 *Phys. Rev. B* **46** 2792
- [24] Williamson W and Lee S A 1991 *Phys. Rev. B* **44** 9853
- [25] Jayaraman A, Kouroulis G A, Cooper A S and Espinosa G P 1990 *J. Phys. Chem.* **94** 1091
- [26] Kruger M B, Williams Q and Jeanloz R 1989 *J. Chem. Phys.* **91** 5910
- [27] Kruger M B and Jeanloz R 1990 *Science* **249** 647
Tse J S and Klug D D 1992 *Science* **255** 1559
- [28] Alba-Simionesco C 1994 *J. Chem. Phys.* **100** 2250
- [29] Köpflinger J, Kasper G and Hunklinger S 2000 *J. Chem. Phys.* **113** 4701
- [30] Hédoux A, Guinet Y, Capet F, Affouard F and Descamps M 2002 *J. Phys.: Condens. Matter* **14** 8725
- [31] Fraczyk L A and Huang Y 2001 *Spectrochim. Acta A* **57** 1061
- [32] Zallen R 1974 *Phys. Rev. B* **9** 4485
- [33] Zallen R and Slade M L 1978 *Phys. Rev. B* **18** 5775